Applied Scientific Research **51:** 411–415, 1993.
F.T.M. Nieuwstadt (ed.), Advances in Turbulence IV.

Rapid Distortion of Turbulent Structures

N.K.-R. KEVLAHAN
Department of Applied Mathematics and Theoretical Physics, University of Cambridge, Silver Street, Cambridge, CB3 9EW

Abstract. A simple two scale rapid distortion model of turbulence is used to investigate the generation of coherent structures and to explain some dynamical effects (vorticity alignment with the intermediate eigenvector of the rate of strain, and vorticity production) which have been observed in recent Direct Numerical Simulations (Vincent & Meneguzzi 1991, Ashurst *et al.* 1987).

A three dimensional homogeneous, isotropic, turbulent velocity field with the Von Karman energy spectrum is generated from random Fourier modes (Kinematic Simulation), and dynamics are added by subjecting this flow to a variety of plane large scale distortions calculated using Rapid Distortion Theory (RDT). Five non-overlapping zones (eddy, donor, convergence, shear and streaming regions) are defined. Eddy, convergence and donor regions increase with the proportion of rotational straining by the large scales, while stream regions increase with irrotational distortion. Shear regions show the largest overall change in volume.

After large scale irrotational straining the small scale vorticity aligns with the *middle* eigenvector of the small scale rate of strain, but with the largest eigenvector of the large scale rate of strain. There is no net production (destruction) of vorticity except under large scale irrotational strain in regions with two positive (negative) eigenvalues of the small scale rate of strain. These vorticity alignment and production results may be deduced analytically from Rapid Distortion Theory by assuming that the initial turbulence is homogeneous and isotropic.

Key words: turbulence – structures – alignment – straining

1. Introduction

Direct Numerical Simulations (DNS) have shown that turbulence dynamics are highly localised and are related to the corresponding fluid structures, e.g. the high intensity vorticity is concentrated into thin vortex tubes (Vincent & Meneguzzi 1991) and vorticity aligns with the middle eigenvector of the rate of strain tensor (Ashurst *et al.* 1987). Two important questions arise from these observations. First, do the turbulence dynamics reinforce this intermittency, thus leading to persistent coherent structures? Secondly, which of these results are related to local scale dynamics, and which to interactions between large and small scales?

The purpose of this investigation is to determine which aspects of the dynamics of turbulence can be accounted for by the simple linear dynamics of RDT. Or, more specifically, what aspects of 'real' turbulence that are not seen in random or Gaussian turbulence may be seen when Gaussian turbulence (generated by Kinematic Simulation, or KS) is subjected to a rapid distortion? An important case where the origin of a dynamical effect is unclear is the alignment of the middle eigenvector (associated with the middle eigenvalue) of the rate of strain tensor with the vorticity. This alignment is *not* seen in Gaussian or random turbulence

(Shtilman *et al.* 1992). Ashurst *et al.* (1987) and Vincent & Meneguzzi (1991) have observed such an alignment in Direct Numerical Simulations and believed it to arise from poorly understood nonlinear effects. Recently Jiménez (1992) has put forward a theory to explain why one might expect to see this alignment in regions where the vorticity is aligned primarily in one direction, however this is a purely kinematic theory and does not explain how such alignments arise. In this paper we provide a possible explanation of some of the DNS results by dividing a turbulent flow into characteristic structure types, and modelling the interaction between the large and small scales as a rapid distortion of the small scales by the large scales.

2. Theory and method

Three-dimensional homogeneous, isotropic turbulence generated by KS is subjected to combinations of rotational and irrotational plane distortions ranging from pure rotation through pure shear to pure irrotational strain. Distortions with large-scale $S+\Omega = 20.0$ and $t = 0.1$ (giving a 'β' ($= \alpha t$) of 2.0) are applied to initial KS flows with both the Von Karman spectrum, $E(k, 0) = 1.196k^4/(0.558 + k^2)^{17/6}$, and exponential spectrum, $E(k, 0) = k^2 \exp(-0.75k^2)$.

The large-scale structures determine the distortion felt by the small-scales. For example, a large-scale eddy would induce a rotational distortion, whereas the regions between eddies would induce irrotational distortions and an intermediate position around an eddy would usually lead to a combination of these effects, i.e. a shear distortion. We put forward a model of turbulence in which the small-scale eddies are advected past the large-scale eddies thereby passing through regions producing a variety of distortions. The effect of these distortions is calculated using RDT. For arbitrary combinations of rotational and irrotational distortion the RDT equations cannot be solved analytically for general initial conditions, so the equations are solved numerically using an adjustable step-size method. A variety of dynamical quantities (eg. vorticity production, alignment of eigenvectors of rate of strain with vorticity, angle between velocity and vorticity) are measured before and after the distortions.

The flow is divided into different structure types using an algorithm we developed based on values of pressure, speed and the parameter Σ defined as,

$$\Sigma = \frac{S_{ij}^2 - \Omega_{ij}^2}{S_{ij}^2 + \Omega_{ij}^2}, \tag{1}$$

where S_{ij} is the rate of strain tensor, and Ω_{ij} is the vorticity tensor. The five basic structure types are: eddy—$\Sigma < -1/3$ and $p < 0$; donor eddies—$\Sigma < -1/3$ and $p > 0$; shear—$-1/3 \leq \Sigma \leq 1/3$; convergence—$\Sigma > 1/3$ and $p > 0$; and streaming— $|u| > u_{\text{RMS}}$ and $|\Omega| < \frac{1}{2}|\Omega|_{\text{RMS}}$, $|S| < \frac{1}{2}|S|_{\text{RMS}}$. (Note that for all regions except streams the level of strain must be above a certain threshold, i.e. $|\Omega| \geq \frac{1}{2}|\Omega|_{\text{RMS}}$, $|S| \geq \frac{1}{2}|S|_{\text{RMS}}$.) Thus eddies are regions of high vorticity with closed streamlines about a low pressure core; donor eddies are regions of

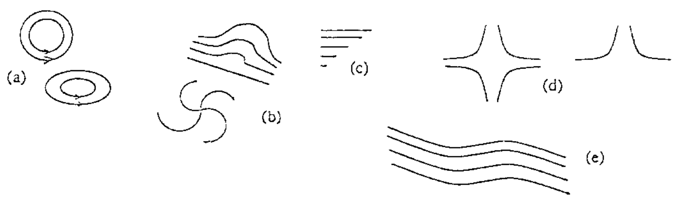

Fig. 1. Schematic diagram of the five structure types. (a) Eddy, (b) donor eddy, (c) shear, (d) convergence, (e) streaming.

high vorticity and positive pressure fluctuation without closed streamlines, shear structures are regions of shear straining; convergence structures are regions of irrotational straining characterised by converging streamlines and positive pressure fluctuation; and stream structures are regions of low deformation and high kinetic energy. This algorithm identifies about 80% of the initial flow. The algorithm differs from than that of Wray & Hunt (1990) in that it is not based on the second invariant, classifies 50% more of the flow, gives consistent identification of the same structures in different flows, defines donor eddies and has a more intuitive definition of shear regions.

3. Results

Under irrotational distortion small-scale vorticity aligns with the intermediate eigenvector of the small-scale rate of strain, but with the large eigenvector of the large-scale (applied) strain. Alignment with the large eigenvector of the applied strain is clearly expected from an examination of the vorticity equation,

$$\frac{D\boldsymbol{\omega}}{Dt} = \boldsymbol{\omega} \cdot (\mathbf{S}^{S-S} + \mathbf{S}^{L-S}) - (\mathbf{U} \cdot \nabla)\boldsymbol{\omega}, \tag{2}$$

where $\mathbf{S}^{S-S}$ is the small-scale rate of strain tensor and $\mathbf{S}^{L-S}$ is the large-scale rate of strain tensor. The less obvious alignment with the middle eigenvector of $\mathbf{S}^{S-S}$ can be shown using an RDT analysis for large time. Neglecting exponentially small terms in time and working in the frame of the eigenvectors of $\mathbf{S}^{L-S}$, one finds that for an irrotational large-scale strain,

$$k^2\mathbf{S}^{S-S} \sim \begin{pmatrix} k_{10}k_{30}\hat{\omega}_{20} & k_{20}k_{30}\hat{\omega}_{20}e^{St} & k_{30}^2\hat{\omega}_{20}e^{2St} \\ k_{20}k_{30}\hat{\omega}_{20}e^{St} & -k_{20}k_{30}\hat{\omega}_{10}e^{2St} & -\frac{1}{2}k_{30}^2\hat{\omega}_{10}e^{3St} \\ k_{30}^2\hat{\omega}_{20}e^{2St} & -\frac{1}{2}k_{30}^2\hat{\omega}_{10}e^{3St} & k_{20}k_{30}\hat{\omega}_{10}e^{2St} \end{pmatrix} \tag{3}$$

where the eigenvalues of $\mathbf{S}^{L-S}$ are $(S, 0, -S)$. For large times (3) has the eigenvalues C, 0, $-C$ (where $C = -\frac{1}{2}k_{30}^2\hat{\omega}_{10}e^{3St}$) with eigenvectors $(0, 1, 1)$, $(1, 0, 0)$, $(0, 1, -1)$ respectively. This shows that the middle eigenvector of $\mathbf{S}^{S-S}$ will align with the large eigenvector of $\mathbf{S}^{L-S}$. Since the small scale vorticity aligns with the large eigenvector of $\mathbf{S}^{L-S}$ (see equation (2)) this shows that the small scale vorticity will align with the *intermediate* eigenvector of $\mathbf{S}^{S-S}$.

Local vorticity production was measured by calculating $\omega_i\omega_j S_{ij}$ which is the source term in the enstrophy equation,

$$\frac{D(\frac{1}{2}\omega^2)}{Dt} = \omega_i\omega_j S_{ij} - \nu\left(\frac{\partial\omega_i}{\partial x_j}\right)^2 . \tag{4}$$

Initially there is no significant vorticity production (Gaussian initial field). Vorticity production is dramatically increased under applied irrotational distortion in regions with a positive intermediate eigenvalue of $\mathbf{S}^{S-S}$, and vorticity is destroyed in regions with a negative intermediate eigenvalue. This result was essentially predicted by Betchov (1956) and can also be deduced from an large time RDT calculation with the assumption that the small scales are initially homogeneous and isotropic. For large times in the frame of the eigenvectors of $\mathbf{S}^{S-S}$ one finds that

$$\omega_i\omega_j S_{ij} = (a\omega_{10}^2 - 2\omega_{20}\omega_{30})e^{2St} \tag{5}$$

where a is the intermediate eigenvalue of $\mathbf{S}^{S-S}$ and S is the large scale rate of strain. However, because of isotropy $< \omega_{20}\omega_{30} >= 0$ and hence

$$< \omega_i\omega_j S_{ij} >=< a\omega_{10}^2 > e^{2St}. \tag{6}$$

Enstrophy will be exponentially created (destroyed) if $a > 0$ ($a < 0$). This destruction of enstrophy in some strained regions and its production in other strained regions (depending on local values of the eigenvalues of $\mathbf{S}^{S-S}$) will eventually lead to a highly intermittent vorticity distribution. Thus, in a turbulent flow where the vorticity is initially evenly distributed, linear straining effects will tend to lead to concentrate vorticity into small regions—thin vortex tubes. Again, we see linear effects largely responsible for a fundamental aspect of turbulence: the highly intermittent distribution of vorticity.

Perpendicular alignment of velocity and vorticity becomes more pronounced after irrotational straining, i.e. nonlinearity is enhanced. The number of 'cigar' regions (negative intermediate eigenvalue) and 'pancake' (positive intermediate eigenvalue) regions remained roughly constant at 50% each under all distortions.

The change in the relative proportion of each of the structures with different types of large-scale distortion is shown in figure 2. Figure 2 shows that the percentage of eddies, convergence and shear regions increases with the proportion of rotational distortion, while the percentage of streams and donor eddies increases with proportion of irrotational distortion. The average percentage of eddies over the range of distortions about equals the initial value, while convergence, shear and donor regions are *suppressed* relative to the initial amount for all, but high rotational distortion. Stream regions, on the other hand, are *increased* relative to the initial value for all distortions except at high rotational distortion. Interestingly, the amount of eddies and shear regions is unaffected by a pure shear distortion. Changes in percentage of convergence regions mirrors the changes in eddy regions. This is expected since convergence regions are associated with the area between

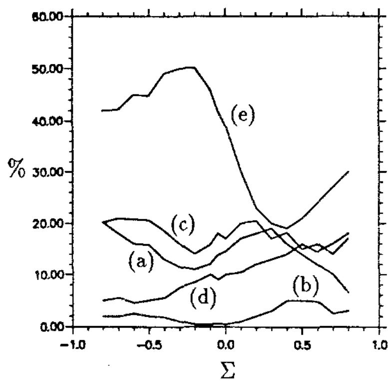

Fig. 2. Percentage change in number of structures as a function of type of applied distortion. $\Sigma = (S - \Omega)/(S + \Omega)$. (a) Eddies, (b) donor eddies, (c) convergence regions, (d) shear regions, (e) stream regions.

eddies. Shear regions undergo the greatest overall change (30%). The changes in the number of structure types with applied distortion was significantly less, but qualitatively the same, for the Von Karman spectrum. This indicates structure is most affected by changes to the small-wavenumber part of the spectrum.

4. Conclusions

In this paper we have shown how some of the dynamical effects observed in DNS of turbulence (i.e. alignment of vorticity with the intermediate eigenvector of the rate of strain tensor, intermittency of vorticity) may arise from simple straining processes. Thus, irrotational straining of the small scales could lead to the creation of long, thin tubes of intense vorticity and to the alignment between vorticity and the intermediate eigenvector of the rate of strain tensor. Both effects have been observed in recent DNS (Vincent & Meneguzzi 1991).

We have also shown how the relative numbers of various structure types (eddies, donors, convergence, shear, streams) changes as a function of the type of applied large scale strain.

References

1. Ashurst, W.T., Kerstein, A.R., Kerr, R.M. & Gibson, C.H. 1987. Alignment of vorticity and scalar gradients with strain rate in simulated Navier-Stokes turbulence. *Phys. Fluids* **30**(8), 2343-2353.
2. Betchov, R. 1956. An inequality concerning the production of vorticity in isotropic turbulence. *J. Fluid Mech.* **1**, 497-504.
3. Jiménez, J. 1992. Kinematic alignment effects in turbulent flows. *Phys. Fluids* A **4** (4), 652-654.
4. Shtilman, L. Spector, M. & Tsinober, A. 1992. On some kinematic versus dynamic properties of homogeneous turbulence. Preprint.
5. Vincent, A. & Meneguzzi, M. 1991. The spatial structure and statistical properties of homogeneous turbulence. *J. Fluid Mech.* **225**, 1-20.
6. Wray, A.A. & Hunt, J.C.R. 1990. Algorithms for classification of turbulent structures. In *Proc. IUTAM Symp.* 1989, *Topological fluid mechanics* (eds. H.K. Moffatt and A. Tsinober), 95-104. Cambridge University Press.